Suspension Performance Analysis of a Half Car Model with a Fluid Inerter

Chen Wang [1], Shichang Han* [1], Jing Na [1], Xian Wang [1], Zhongcheng Qiu [1]

1. Faculty of mechanical and electrical engineering, Kunming University of Science and Technology, Kunming, 650500,China

E-mail: han_shichang@163.com

Abstract: As a new type of vibration isolation component, inerter has great potential in improving the performance of vibration isolation system. In this paper, a half car model is taken as the research object, and three suspension structure models with inerter are studied. Particle swarm optimization algorithm is used to optimize the parameters of inerter suspension. The performances of the three inerter suspensions are compared with those of the traditional suspension in terms of body acceleration and pitching angular acceleration. The simulation results show that compared with the traditional suspension, the performance of the suspension system with inerter has been significantly improved. In addition, the dynamic model of fluid inerter including friction force, parasitic damping force and inertial force is established, and the nonlinearity of fluid inerter is analyzed in frequency domain and time domain.

Key Words: half car model, vehicle suspension, fluid inerter, nonlinear, performance

1 INTRODUCTION

Suspension is an important part of vehicle chassis system, which has a direct and important impact on the vehicle handling stability, riding comfort and driving safety [1]. With the development of automobile industry, semi-active suspension and active suspension have been brought out. However, the high cost, complex control and large energy consumption limit the further promotion of semi-active and active suspension [2] [3]. In contrast, passive suspension has the advantages of mature theory, simple structure, reliable performance and low cost. While it is widely used in the automotive field currently, study on passive suspension to improve its performance still gets a significant meaning. Traditional passive suspension usually consists of springs and dampers. Since 2002, the author of [4] developed a mechanical element which has similar physical properties to the mass element. The work [5] [6] [7] showed that inerter is widely used in the fields of train, aerospace, construction, automobile and so on. The study [8] [9] studied the application of inerter in vehicle engineering in the quarter vehicle model. The paper [10] took a quarter car as the research object and analyzes the ball screw inerter. The article [11] studied the nonlinear factors of fluid inerter, and brought it into the quarter car model to analyze the performance of suspension with a fluid inerter. In 2013, the author of [12] proposed a kind of fluid inerter with liquid as medium and helix tube as "flywheel". Because of the backlash and other reasons, the influence of nonlinear factors on the mechanical properties of a mechanical inerter can not be ignored. Compared with the mechanical inerter,

fluid inerter not only has the advantages of simple structure, large bearing capacity and low processing cost, but also can avoid the fracture and backlash problems existing in the mechanical inerter [13]. Meanwhile, the hydraulic system has less friction and is easy to be arranged. Thus, it can be widely used in vibration isolation of large vehicles and buildings.

Most of the suspension research with inerter is based on a simplified quarter vehicle model. however, the pitch angle acceleration can not be reflected in a quarter vehicle model, which is also an important indicator to the performance of suspension, vehicle comfort is also effected by the pitch angle acceleration too. In this paper, the half car is taken as the model, three kinds of suspension with inerter are introduced, and the mathematical model of fluid inerter is established. Both the theoretical inerters and fluid inerters with nonlear factors are used when the vibration isolation performance is analyzed under the random road input conditions. The influence of its nonlinear factors is analyzed at last.

2 INERTER SUSPENSION AND MODELING

2.1 Vertical dynamic model of half car suspension

In this paper, a half car system is studied. As shown in Fig. 1, m_v and I_v are the mass of the vehicle body and the mass moment of inertia for the pitch motion; m_f and m_r are the upsprung masses of front and rear wheels; S_f and S_r are the front and rear suspension systems. a and b define the distances between the suspension system to the vehicle body center, and z_{w1} and z_{w2} are the pavement inputs.

In Fig.1, dynamics of the vertical model with suspensions can be obtained based on Newton's law:

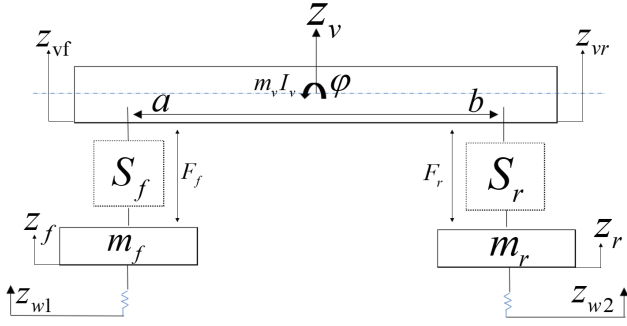$$m_v\ddot{z}_v + F_f + F_r = 0 \qquad (1)$$
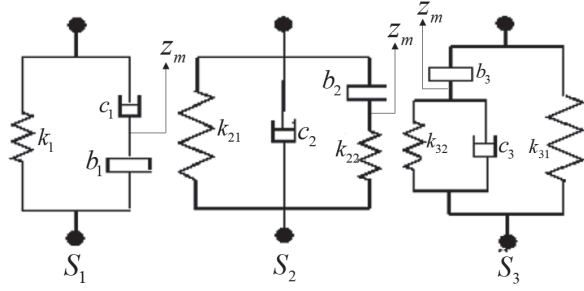
Figure 1: half car model

Figure 2: Suspension layouts

where F_f is the force of the front suspension and F_r is the force of the rear suspension.

Pitch angle motion:

$$I_v \ddot{\varphi}_v + aF_f - bF_r = 0 \qquad (2)$$

Elasticity forces of the tires:

$$\begin{cases} m_f \ddot{z}_f + k_{tf}(z_f - z_{w1}) - F_f = 0 \\ m_f \ddot{z}_r + k_{tr}(z_r - z_{w2}) - F_r = 0 \end{cases} \qquad (3)$$

The relationship between the pitching angle of the car body and the vertical displacement of the car body z_v is as follows:

$$\begin{cases} z_{vf} = z_v - a\varphi \\ z_{vr} = z_v + b\varphi \end{cases} \qquad (4)$$

2.2 Suspension with inerter

In this section, three suspension structures with inerter are introduced [14]. They have the characteristics of simple structure are easy to industrialize. As Fig.2, In S_1 the inerter b_1 is in series with the damping c_1, and then they are connected with spring k_1 in parallel. S_2 are constructed by connecting in parallel the damping c_2, main spring k_{21} and the inerter b_2 while there is an auxiliary spring k_{22} connecting in series with b_2. The inerter b_3 connected in series with the auxiliary spring k_{32} and damping c_3 and then connected in parallel with main spring k_{31} to form suspension S_3. what's more, the traditional suspension, which is modeled by a spring in parallel with a damper, is marked as S_0 to be the comparing group.

According to the different suspension layouts, the expressions of vertical force of traditional suspension S_0 and inerter suspension S_1, S_2 and S_3 are as follows:
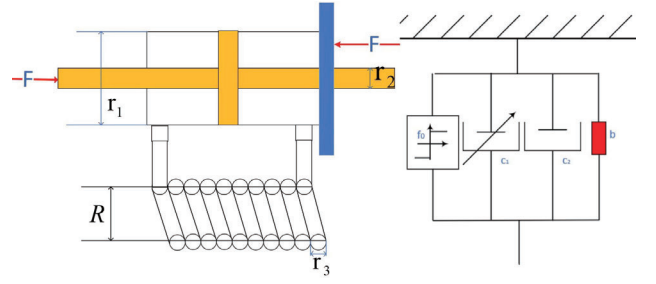

Figure 3: fulid inerter

$$S_0 \begin{cases} F_f = k_{0f}(z_{vf} - z_f) + c_{0f}(\dot{z}_{vf} - \dot{z}_f) \\ F_r = k_{0r}(z_{vr} - z_r) + c_{0r}(\dot{z}_{vr} - \dot{z}_r) \end{cases} \qquad (5)$$

$$S_1 \begin{cases} F_f = k_{1f}(z_{vf} - z_f) + F_{b1f} \\ F_r = k_{1r}(z_{vr} - z_r) + F_{b1r} \end{cases} \qquad (6)$$

$$S_2 \begin{cases} F_f = k_{21f}(z_{vf} - z_f) + c_{2f}(z_{vf} - z_f) + F_{b2f} \\ F_r = k_{21r}(z_{vr} - z_r) + c_{2r}(z_{vr} - z_r) + F_{b2r} \end{cases} \qquad (7)$$

$$S_3 \begin{cases} F_f = k_{31f}(z_{vf} - z_f) + F_{b2f} \\ F_r = k_{31r}(z_{vr} - z_r) + F_{b3r} \end{cases} \qquad (8)$$

where z_m is interstage displacement. In the series structure, the upper and lower forces on the interstage displacement z_m are the same. F_b is the force at both ends of the inerter which shown in formula(9) and (10).

3 MATHEMATICAL MODEL OF FLUID IN-ERTER

The working principle of the fluid inerter: the helix-tube is wrapped on the outer surface of the cylinder, and the oil inlet and outlet of the hydraulic cylinder are respectively connected with the two ends of the helix tube. The piston pushes the oil in the hydraulic cylinder from one chamber of the hydraulic cylinder to another through the helix-tube. The oil flows in the spiral tube produces inertia, and the inertia force is proportional to the relative acceleration at both ends of the piston rod.

As in Fig.3, the force of the fluid inerter is mainly composed of three parts. The first part is the inertial force in the fluid inerter. The second part is the parasitic damping force produced by the fluid moving in the hydraulic cylinder and the helix tube, which is the main nonlinear factor. The last part is the seal of friction force.

Finally, the nonlinear model of the fluid inerter can be simplified as:

$$F_b = b\ddot{x} + c_1 \dot{x}^2 + c_2 \dot{x} + f_0 sign(\dot{x}) \qquad (9)$$

where b is inertance coefficient, c_1 and c_2 is parasitic damping coefficient and f_0 is friction.

In order to study the main performance of the fluid inerter, the following assumptions are made [12]：

- The device is completely sealed without oil leakage, which meets the volume conservation;

- The oil is continuous and incompressible, and its density remains unchanged;

- The effects of heat energy, potential energy dissipation and temperature on oil properties are ignored.

3.1 Inertance coefficient

Assume that the radius of the piston rod is r_1, the radius of piston is r_2, the diameter of the helix tube is r_3. The effective area of the piston is A_1, the sectional area is A_2, bend radius of the helix tube is R, and the total length is l. ρ and μ is the density and viscosity of the liquid.

Suppose x is the relative displacement between the piston and hydraulic cylinder, and the force on the piston rod is F, then we have:

$$F = b\ddot{x} \tag{10}$$

Assuming that the average velocity of the oil in the helix tube is u, according to the conservation of volume, we can get the following results:

$$\dot{x}A_1 = uA_2 \tag{11}$$

According to the conservation of energy, where

$$E = \frac{1}{2}mu^2 = \frac{\rho A_2 l u^2}{2} \tag{12}$$

Meanwhile, the energy stored in the container is as follows:

$$E = \frac{b\dot{x}^2}{2} \tag{13}$$

So, the inertance coefficient is obtained:

$$b = \rho l \frac{A_1^2}{A_2} \tag{14}$$

3.2 Parasitic damping coefficient

The main cause of damping force in the fluid inerter is the pressure loss of oil. According to the results of Rodman and Trenc [15], the damping force in the helix tube is calculated:

$$F_h = 0.03426\frac{2\rho l u^2}{\sqrt{D_h R}}A_1 + 17.54\frac{2\mu l u}{D_h^2}A_1 \tag{15}$$

where D_h is hydraulic diameter.

According to Massey's empirical formula [16], the pressure losses at the inlet and outlet are as follows:

$$\Delta p_{in} = \frac{\rho u^2}{4} \tag{16}$$

$$\Delta p_{out} = \frac{\rho u^2}{2} \tag{17}$$

The shear friction between the piston and the hydraulic cylinder will also lead to pressure loss [12]. Suppose A_f is the contact area between the piston and the hydraulic cylinder and Δr is its gap. The shear friction can be calculated:

$$F_s = \frac{\mu A_f \dot{x}}{\Delta r} \tag{18}$$

Table 1: Classification standard of pavement roughness

Pavement grade	pavement roughness classification		
	$G_q(n_0)/10^{-6}m^3, n_0 = 0.1m^{-1}$		
	lower limit	geometric mean	upper limit
A	8	16	32
B	32	64	128
C	128	256	512
D	512	1024	2048
E	2048	4096	8192
F	8192	16384	32768
G	32768	65536	131072
H	131072	262144	524288

The shear friction is compared with the damping force in the spiral tube:

$$\frac{F_s}{17.54\frac{2\mu l u}{D_h^2}A_1} = \frac{A_f A_2}{A_1^2}(\frac{D_h^2}{35.08l\Delta r}) \tag{19}$$

The friction force of F_s is much less than that of damping force in helix tube, so the shear friction can be ignored [12]. The results show that the damping force caused by pressure loss between inlet and outlet is very small compared with F_h [17]. Therefore, the total damping force F_d can be expressed by the approximate value of the damping force F_h in the helix tube [12]:

$$F_d = 0.03426\frac{2\rho l A_1}{\sqrt{D_h R}}(\frac{A_1}{A_2})^2\dot{x}^2 + 17.54\frac{2\mu l A_1}{D_h^2}(\frac{A_1}{A_2})\dot{x} \tag{20}$$

The parasitic damping coefficient of fluid inerter are obtained:

$$\begin{cases} c_1 = 0.03426\frac{2\rho l A_1}{\sqrt{D_h R}}(\frac{A_1}{A_2})^2 \\ c_2 = 17.54\frac{2\mu l A_1}{D_h^2}(\frac{A_1}{A_2}) \end{cases} \tag{21}$$

4 ROAD MODEL AND INERTER SUSPENSION PARAMETER OPTIMIZATION

4.1 Random pavement model

The road roughness can be divided into eight grades according to the power spectral density, such as grade A to H [18] [19], as shown in Table 1

The fitting formula of pavement power spectral density recommended by international standard IOS 8608 and national standard GB 7031-86 is as follows:

$$G_q(n) = G_q(n_0)(\frac{n}{n_0})^{-W} \tag{22}$$

where, $G_q(n_0)$ is Roughness coefficient of pavement. It is the road power spectral density value under the reference space frequency n_0. And n represents the number of wavelengths per meter of length, which is the reciprocal of the wavelengths, and is called the spatial frequency. W is the frequency index, which represents the slope of the oblique line on the double logarithmic coordinate, and determines the structure of the road power spectral density.

According to [20], the time domain model of road roughness with filtered white noise is obtained as follows:

$$\dot{z}_{\mathrm{g}}(t) = -2\pi n_1 u z_g(t) + 2\pi n_0 \sqrt{G_q(n_0)u}\omega(t) \qquad (23)$$

In this paper, the vibration isolation effect of suspension structure is studied by using the common road conditions of class A and C with speed of 10m/s and 20m/s as excitation.

4.2 Parameter optimization of suspension system

Particle swarm optimization (PSO) is a kind of random search algorithm developed by simulating the foraging behavior of birds. It is of strong optimization ability and has wide range of applications. In order to further improve the performance of vehicle suspension, PSO algorithm is used to optimize the parameters of vehicle suspension. Considering the body acceleration, pitch angular acceleration, suspension working space and tire load as indicators of optimization, However, the above evaluation indexes are often contradictory. Therefore, in the process of suspension system design, these contradictory performance requirements must be considered [21]. In order to compare the performance differences between different suspension systems, it is reasonable to analyze and compare the body acceleration, pitch angular acceleration and tire dynamic load under the condition of ensuring the suspension dynamic travel. Then the fitness function is determined as follows:

$$J_{min} = w_1 * \frac{A}{A_{past}} + w_2 * \frac{F}{F_{past}} + w_3 * \frac{S_f}{S_{fpast}} \\ + w_3 * \frac{S_r}{S_{rpast}} + w_4 * \frac{L_f}{L_{fpast}} + w_4 * \frac{L_r}{L_{rpast}} \qquad (24)$$

where, A is the root mean square acceleration of half car body, and A_{past} is the root mean square acceleration of half car body with traditional suspension. F, S and L are root mean square of pitch angular acceleration, suspension working space and tire load of the half car. According to the importance of different indicators, the indicators are weighted as [22]. where $w_1 = 0.4$, $w_2 = 0.2$, $w_3 = 0.1$ and $w_4 = 0.1$ are selected.

The range of relevant parameters is set:

$$\begin{cases} 10000N/m \le k_{n1} \le 100000N/m \\ 1000N/m \le k_{n2} \le 100000N/m \\ 500Ns/m \le c_n \le 5000Ns/m \\ 50kg \le b_n \le 800kg \end{cases}$$

The speed of 10m/s on grade A pavement is the most common speed, which is used as the input for parameter optimization. The relevant parameters of the half car model are shown in table 2:

The MATLAB software and PSO algorithm are used to optimize the parameters of three kinds of suspension S_1, S_2 and S_3. The final parameters are shown in Table 3.

The inerter is designed according to the content of Section 3. The hydraulic cylinder with a diameter of $r_1 = 63mm$ is selected here, the diameter of the piston is $r_2 = 25mm$, the bend radius of the helix tube is $R = 0.05m$, and the inner diameter of the helix tube is $r_3 = 2.5mm$. Finally, the parameters of the fluid inerter are calculated:

Table 2: Half car parameters

Parameter	value
$I_v(kg \cdot m^2)$	$1222kg \cdot m^2$
$m_v(kg)$	690
$m_f(kg)$	40
$m_r(kg)$	45
$a(m)$	1.3
$b(m)$	1.5

Table 3: parameters optimization results

S_0	$k_f = 17000N/m$ $c_f = 2500Ns/m$ $k_r = 22000N/m$ $c_r = 2000Ns/m$	S_1	$k_{1f} = 10000N/m$ $c_{1f} = 1759Ns/m$ $b_{1f} = 800kg$ $k_{1r} = 10000N/m$ $c_{1r} = 1325Ns/m$ $b_{1r} = 455kg$
S_2	$k_{21f} = 10000N/m$ $k_{22f} = 1000N/m$ $c_{2f} = 1572Ns/m$ $b_{2f} = 800kg$ $k_{21r} = 10000N/m$ $k_{22r} = 1000N/m$ $c_{2r} = 1656Ns/m$ $b_{2r} = 800g$	S_3	$k_{31f} = 10000N/m$ $k_{32f} = 12469N/m$ $c_{3f} = 1737Ns/m$ $b_{3f} = 343kg$ $k_{31r} = 10000N/m$ $k_{32r} = 1000N/m$ $c_{3r} = 1588Ns/m$ $b_{3r} = 445kg$

5 SYSTEM PERFORMANCE ANALYSIS

In this Section, three different suspensions are put into the half car model. We introduce four different pavement conditions, as described in Section 4.1. Vehicle bady acceleration and pitch angular acceleration are chosen as the performance indicators since the space is limited. The performance of all suspensions above under different road conditions is analyzed.

5.1 Time domain analysis

Vehicle body acceleration and pitch angular acceleration of half car system are two important indexes. The performance of suspension will be analyzed in the time domain and frequency domain.

Fig.4 shows the body acceleration performance of a half car equipped with four kinds of suspensions under four road conditions. It can be seen from the figure that compared with the traditional suspension, the three kinds of suspension with fluid inerter have a certain degree of improvement in vehicle body acceleration.

The root mean square of the acceleration of vehicle body with theoretical inerter and fluid inerter under is calculated. It can be seen from Table 5 that under the four road conditions, both theoretical inerter suspension $S_{1,2,3}$ and fluid

Table 4: Parameters of fluid inerter

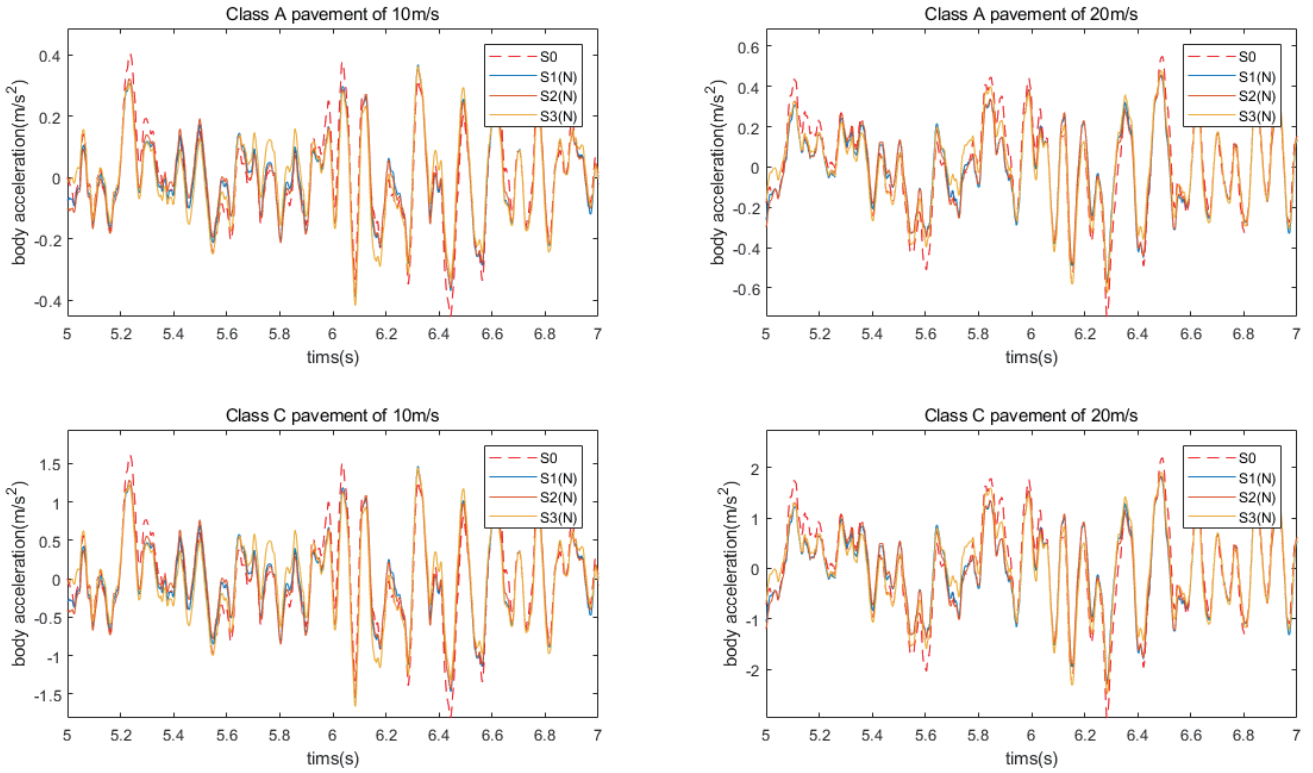|	
$b = 800$	$c_1 = 2500(Ns/m)^2$ $c_2 = 4.653 * 10^5 Ns/m$
$b = 471$	$c_1 = 1325(Ns/m)^2$ $c_2 = 2.734 * 10^5 Ns/m$
$b = 361$	$c_1 = 1015(Ns/m)^2$ $c_2 = 2.094 * 10^5 Ns/m$

Figure 4: Vehicle bady acceleration of different pavement conditions

Table 5: RMS of bady acceleration (m/s^2)

	A10	A20	C10	C20
S_0	0.1613	0.2340	0.6450	0.9359
S_1	0.1456	0.1976	0.5824	0.7905
$S_{1(N)}$	0.1471	0.2024	0.5892	0.8094
S_2	0.1485	0.2040	0.5936	0.8161
$S_{2(N)}$	0.1473	0.2026	0.5894	0.8104
S_3	0.1471	0.1950	0.5883	0.7801
$S_{3(N)}$	0.1484	0.2093	0.5943	0.8371

where A10 represents A-level road surface and 10m/s speed. So are the A20, C10 and C20. S_1 is theoretical inerter suspension, $S_{1(N)}$ is fluid inerter suspension with nonlinearity. SO are the S_2, $S_{2(N)}$, S_3, $S_{3(N)}$.

Table 6: RMS of pitch angular acceleration(rad/s^2)

	A10	A20	C10	C20
S_0	0.1442	0.2072	0.5767	0.8300
S_1	0.1147	0.1705	0.4588	0.6819
$S_{1(N)}$	0.1178	0.1732	0.4718	0.6930
S_2	0.1392	0.1817	0.5566	0.7268
$S_{2(N)}$	0.1362	0.1801	0.5448	0.7203
S_3	0.1166	0.1763	0.4606	0.7053
$S_{3(N)}$	0.1270	0.1822	0.5086	0.7288

inerter suspension $S_{1(N),2(N),3(N)}$ have good performance compared with the traditional suspension in the vehicle body acceleration index. The nonlinearity of $S_{1(N)}$ and $S_{3(N)}$ suspension deteriorates the performance comparing to S_1 and S_3 .

It can be seen from the Fig.5 that suspension with fluid inerter can also be effectively restrained pitch angular acceleration.

Table 6 calculates the root mean square values of pitch angular acceleration under four road conditions. The conclusion is the same as that of vehicle acceleration, which shows both theoretical and fluid inerters can improve pitch angular acceleration while the nonlinearity of $S_{1(N)}$ and $S_{3(N)}$ suspension deteriorates the performance.

5.2 Frequency domain analysis

In this Fig.6 , the frequency domain comparison between three kinds of fluid inerter suspension and the traditional suspension is shown. In the index of vehicle body acceleration, the peak value of power spectrum is lower than that of traditional suspension, especially near 2Hz, which means suspensions with inerter can show an restraining effect in this frequency.

As shown in Fig.7, nonlinearity of different layouts is compared with the index of body acceleration. The results show that the nonlinear factors of $S_{1(N)}$ and $S_{3(N)}$ bring the influence in a frequency band of 0 to 3Hz, while the nonlinear factor of $S_{2(N)}$ suspension gives few influence in the same frequency band.

As shown in Fig.8, the frequency domain analysis of the pitch angular acceleration with traditional suspension and three kinds of fluid inerter suspension is made. The results show that compared with the traditional suspension, benefits form the suspensions with fluid inerter turn out at the frequency band of 2 to 7hz.

In Fig.9,taking the pitch angular acceleration as the evaluation index, the nonlinear factors of fluid inerter are analyzed in the frequency domain. The results show that the nonlinearity of $S_{1(N)}$ and $S_{3(N)}$ deteriorates at low frequency, while $S_{2(N)}$ optimizes it.
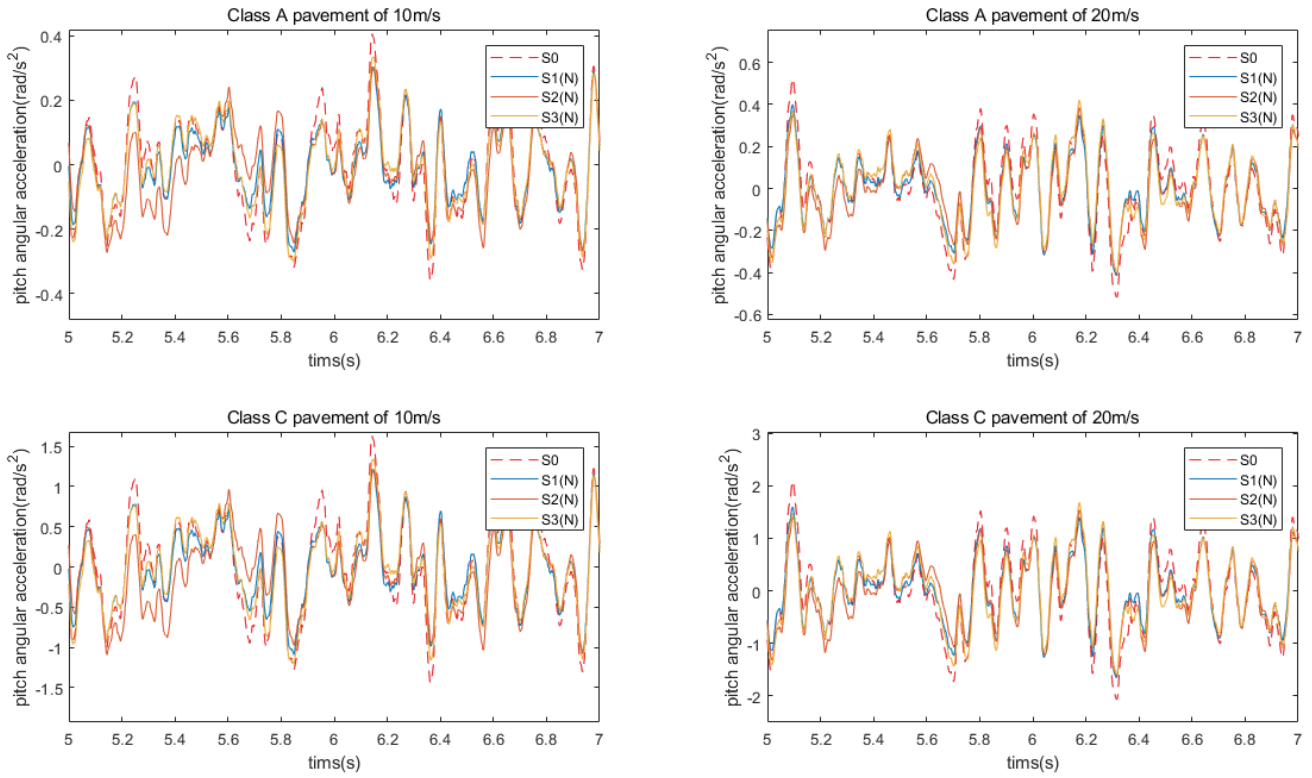
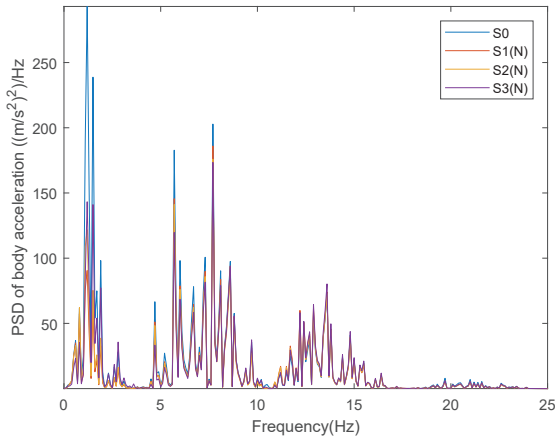Figure 5: Vehicle pitch angular acceleration of different pavement conditions

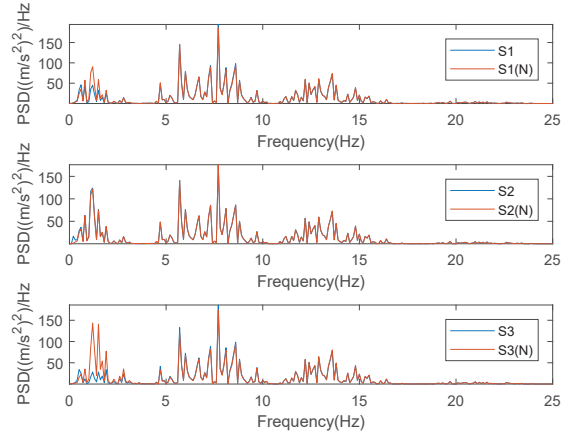Figure 6: Frequecy domain analysis for bady acceleration

Figure 7: Frequecy domain analysis for bady acceleration

The nonlinearity of fluid inerter is mainly caused by damping. And fluid inerter can be regarded as the form of parallel connection of a inerter and a parasitic damping. According to the simulation results, the influence of nonlinear factors is mainly concentrated in low frequency. The performance of $S_{1(N)}$ and $S_{3(N)}$ suspension structure is deteriorated, while $S_{2(N)}$ structure is optimized.

6 CONCLUSION

In this paper, the vibration isolation performance of three kinds of suspensions with inerter is studied based on a half car model. The parameters of suspension are optimized by PSO algorithm. The vehicle body acceleration and pitch angle acceleration are used as evaluation indexes to com-

pare with traditional suspension. Under the input of four different conditions, the vehicle acceleration and pitch angle acceleration are analyzed in time domain and frequency domain.

With the arguments above, we can safely come to the conclusion that:

(1) Compared with the traditional suspension, the performance of the three suspension with inerter has been improved in terms of body acceleration and pitch angular acceleration. Under the road condition of 20m/s on grade C pavement. Compared with traditional suspension, the vehicle body acceleration and pitch angular acceleration of $S_{1(N)}$ suspension increased by 13.5% and 16.5%. the $S_{2(N)}$ suspension promoted 13.4% and 13.2%. And the
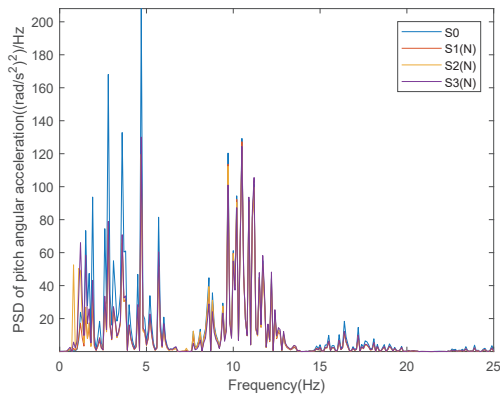
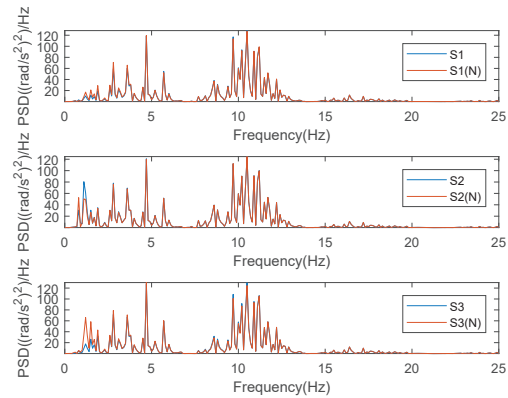Figure 8: Frequecy domain analysis for pitch angular acceleration

Figure 9: Frequecy domain analysis for pitch angular acceleration

$S_{3(N)}$ suspension improved 10.6% and 12.2%.

(2) The fluid flows in the helix tube to form the 'liquid flywheel' effect. Under the influence of damping and nonlinear factors, it still has a good restrain effect.

(3)In the simulation, the nonlinear factors of fluid inerter mainly affect the performance of low frequency.

REFERENCES

[1] M. Mahmoodabadi, F. Farhadi, and S. Sampour, "Firefly algorithm based optimum design of vehicle suspension systems," *International Journal of Dynamics and Control*, vol. 7, no. 1, pp. 134–146, 2019.

[2] H. Jiang, G. Jiantao, and Z. Xiaoliang, "Study on co-simulation of vehicle suspension system employing inerter based on virtual protoype model," *Journal of Vibration and Shock*, vol. 7, no. 12, p. 51, 2010.

[3] R. Wang, L. Chen, H. Jiang, and X. Zhang, "Fuzzy dynamic model and neural network control of semi-active suspension," *Journal of Jiangsu University (natural science edition)*, vol. 1, 2009.

[4] M. C. Smith, "Synthesis of mechanical networks: the inerter," *IEEE Transactions on automatic control*, vol. 47, no. 10, pp. 1648–1662, 2002.

[5] F.-C. Wang and W.-J. Su, "Impact of inerter nonlinearities on vehicle suspension control," *Vehicle system dynamics*, vol. 46, no. 7, pp. 575–595, 2008.

[6] X. Sun, L. Chen, S. Wang, and X. Zhang, "Research on performance benefits in railway vehicle suspension employing inerter," *Journal of the China railway socitty*, vol. 50, no. 7, pp. 32–38, 2017.

[7] I. Lazar, S. Neild, and D. Wagg, "Using an inerter-based device for structural vibration suppression," *Earthquake Engineering & Structural Dynamics*, vol. 43, no. 8, pp. 1129–1147, 2014.

[8] L. Chen, X. Yang, R. Wang, C. Huang, and Y. Shen, "Design and performance study of vehicle passive suspension based on two-element inerter-spring-damper structure vibration isolation mechanism," *Journal of Vibration and Shock*, vol. 32, no. 6, pp. 90–95, 2013.

[9] L. Chen, X. Yang, R. Wang, C. Huang, and Y. Shen, "A study on the performances of vehicle passive suspension with modified inerter-spring-damper three-element structure," *Automotive Engineering*, vol. 36, no. 3, pp. 340–345, 2014.

[10] F.-C. Wang and H.-A. Chan, "Vehicle suspensions with a mechatronic network strut," *Vehicle System Dynamics*, vol. 49, no. 5, pp. 811–830, 2011.

[11] Y. Shen, L. Chen, Y. Liu, and X. Zhang, "Influence of fluid inerter nonlinearities on vehicle suspension performance," *Advances in Mechanical Engineering*, vol. 9, no. 11, p. 16, 2017.

[12] S. Swift, M. C. Smith, A. Glover, C. Papageorgiou, B. Gartner, and N. E. Houghton, "Design and modelling of a fluid inerter," *International Journal of Control*, vol. 86, no. 11, pp. 2035–2051, 2013.

[13] X. Liu, J. Z. Jiang, B. Titurus, and A. Harrison, "Model identification methodology for fluid-based inerters," *Mechanical Systems and Signal Processing*, vol. 106, pp. 479–494, 2018.

[14] T. Jiang, L. Chen, and X. Zhang, "Suspension performance analysis based on combination of inerter-spring-damper," *Journal of Chongqing University of Technology (Natural Science)*, vol. 12, pp. 7–17, 2014.

[15] S. Rodman and F. Trenc, "Pressure drop of laminar oil-flow in curved rectangular channels," *Experimental thermal and fluid science*, vol. 26, no. 1, pp. 25–32, 2002.

[16] B. S. Massey and J. Ward-Smith, *Mechanics of fluids*, vol. 1. Crc Press, 1998.

[17] X. Liu, *Fluid inerter based vibration suppression: modelling methodology*. PhD thesis, University of Bristol, 2019.

[18] I. ISO, "Mechanical vibration—road surface profiles—reporting of measured data," 1995.

[19] M. Agostinacchio, D. Ciampa, and S. Olita, "The vibrations induced by surface irregularities in road pavements–a matlab® approach," *European Transport Research Review*, vol. 6, no. 3, pp. 267–275, 2014.

[20] J. Yin, J. Chen, and Y. Liu, "Simulation method of road excitation in time domain using filtered white noise and dynamic analysis of suspension," *Journal of Tongji University*, vol. 45, pp. 398–407, 2017.

[21] L. Zhang and J. Zhang, "A research on comprehensive performance evaluation method for vehicle suspension system," *Automotive Engineering*, vol. 38, pp. 1494–1499, 2016.

[22] H. Zhang, "Simulation and test research of hydropneumatic isd suspension," Master's thesis, Jiangsu University, 2017.